J Electroceram (2006) 16:593–598
DOI 10.1007/s10832-006-9925-x

# Influence of Au particles on the photocurrent of $TiO_2$ films

**Xiaoping Hu · Daniel J. Blackwood**



**Abstract** Au/$TiO_2$ composite films were employed in an attempt to improve the photon-electron conversion efficiency of $TiO_2$ film in the visible region, using the surface plasma resonance (SPR) of Au nanoparticles. For investigating the relationship between SPR of Au particle and photocurrent of $TiO_2$ film, a series of Au/$TiO_2$ films with different Au concentrations were synthesized by sol-gel method. Results of studies on the influence of Au particle size on crystallization of $TiO_2$ film, UV-vis absorption and photocurrents generated are discussed. It was shown that SPR performance of the Au nanoparticles was not only related to their size, but also to their distribution in the $TiO_2$ matrix. Even in $TiO_2$ films with large Au particle sizes (100 nm), SPR in visible region was still observed. However, this SPR performance did not contribute to the photon-electron conversion of $TiO_2$ film in the visible region. Contrarily, embedded Au nanoparticles depressed the photocurrent generated by the $TiO_2$ film in UV region. The reason for this decrease is thought to be partly due to the Au simply blocking some of the light and partly because the extent of crystallization of $TiO_2$ decreased with high Au levels.

**Keywords** Au/$TiO_2$ nanocomposite · Photocurrent · SPR

## 1 Introduction

The introduction of Au nanoparticles into $TiO_2$ films has been attractive for its unique optical and photocatalysis properties in improving the efficiency of splitting water and oxidizing CO [1–3]. In recent years, the enhancement of photon-electron conversion of dye-sensitized $TiO_2$ solar cell (DSSC) by Au nanoparticles has also been studied. However, most of these works focused on the influence of nanosize Au particles on the dye-sensitization [4]. Few works considered the relationship between photocurrent and unique optical absorption of Au nanoparticles in the visible region, where $TiO_2$ shows low photon-electron conversion due to its large bandgap. However, Au particles embedded in a $TiO_2$ dielectric matrix show obvious surface plasma resonance (SPR) in the visible region.

In this work, the influence of the particle size of Au nanoparticles on the photon-electron conversion of $TiO_2$ film was investigated by the SPR performance and photocurrent of Au/$TiO_2$ film with different Au concentrations. Previous works reported that porous structures can improve photocurrent, by enlarging the surface area of dye-sensitization [1–5]. Since the aim of the present study was to investigate the influence of Au nanoparticles, all films were synthesized in compact and smooth surface, thus excluding the influence from film structure on the photocurrent.

## 2 Experimental

Au/$TiO_2$ films containing different Au concentrations were deposited at room temperature by sol-gel method on quartz substrates, for optical absorption measurement, and on ITO conductive glass substrates, for photocurrent measurement. The $TiO_2$ precursor was prepared from Titanium (IV) isopropoxide (>98%; Acrons), nitric acid (69.0–70.0%; Baker), absolute alcohol (>99.8%; Merck) and 4 MΩ deionizer water. The ratio of components in precursor solutions followed the method proposed by Takahashi et al. [5], i.e. $Ti(OC_3H_7)_4$:$C_2H_5OH$:$H_2O$:$HNO_3$ = 1 : 20 :

X. Hu · D. J. Blackwood (✉)
Department of Materials Science & Engineering,
National University of Singapore, Singapore 117576
e-mail: msedjb@nus.edu.sg

**Table 1** Chemical compositions of the composites determined by EDX

| Sample | Au : Ti (at%) | Au (at%) |
|---|---|---|
| 1% Au/$TiO_2$ | 0.009 : 1 | 0.88 |
| 5% Au/$TiO_2$ | 0.025 : 1 | 2.4 |
| 10% Au/$TiO_2$ | 0.054 : 1 | 5.4 |
| 25% Au/$TiO_2$ | 0.33 : 1 | 24.8 |
| 50% Au/$TiO_2$ | 0.50 : 1 | 33.2 |

1 : 0.2. Preparation was carried out in a glove box to control the hydrolysis. After ageing for 24 h, this precursor solution was mixed with hydrogen tetrachloroaurate (III), trihydrate ($HAuCl_4 \cdot 3H_2O$, 99.9%; Aldrich) at 1%, 10%, 20%, 25% and 50% atomic ratios (at%) of Au/Ti. Films were deposited by spin-coating at 3000 rpm onto fused quartz glass substrates. The film thickness, as determined by cross-section measurement under a scanning electron microscopy (SEM), varied from 80 to 120 nm. After deposition, composite films were given a pre-treatment process at 200°C on a hotplate, whilst post deposition annealing was carried out at 500°C in air for 30 min.

The chemical composition of the films was derived from the Energy Dispersive X-ray Detector (EDX). Microstructures were characterized and particle sizes determined by means of transmission electron microscopy (TEM, JEM 300C JEOL). Crystallographic structures were determined by both electron and X-ray diffraction (XRD) measured in the grazing incidence configuration (GID) on an X'Pert MPD Philips diffractometer. Optical properties of the deposited thin films were studied with a UV-vis spectrophotometer (UV1601, Shimadzu) in the range of 200 to 800 nm at room temperature. Photocurrent measurements were carried in a three-electrode cell consisting of dye-sensitized Au/$TiO_2$ composite film as photoanode, Pt mesh as counter electrode, and Saturated Calomel reference Electrode (SCE) as reference electrode in 0.1 M $Na_2SO_4$ solution, with an Oriel monochromator with a 450 W Xe lamp as the light source.

## 3 Results and discussion

### 3.1 Crystallization of composite film

Table 1 shows the composition of the films as determined by EDX. It can be seen that the measured Au levels were lower than the designed levels. This may because of the deposition method, spin-coating, which may lead to a loss of the heavier Au particles due to the higher centrifugal force acting on them compared to the lighter $TiO_2$.

After the 200°C pre-treatment XRD (Fig. 1(a)) only reveals peaks associated with the FCC structured nanopartilces, the broad hump at low angles was due to the amorphous nature of the fused quartz glass substrate. With increasing Au concentration the intensity of the peaks became stronger. The size of the Au particles was evaluated by Scherrer's equation [6], and particle size was varied from 13 to 23 nm. After 500°C sintering, $TiO_2$ was crystallized, and the XRD peaks of the Au particles became sharper. Figure 1(b) shows that $TiO_2$ crystallization weakened with increasing Au concentration. Since the strongest Au peak overlapped with a strong $TiO_2$ peak, once $TiO_2$ crystallization occurred Scherrer's equation was not suitable to evaluate Au particle size. Therefore, Au particle size was determined by TEM. From the TEM plain view images shown in Fig. 2, Au particle size changed from about 10 nm in 1 at% Au/$TiO_2$ composite film to about 100 nm in 50 at% Au/$TiO_2$ composite film. It can also be seen that the $TiO_2$ diffraction pattern changed from a dotted ring to a smooth ring, indicating that $TiO_2$ crystallization decreased with increasing Au concentration. Figure 3 shows the statistical Au particle sizes of the various films.

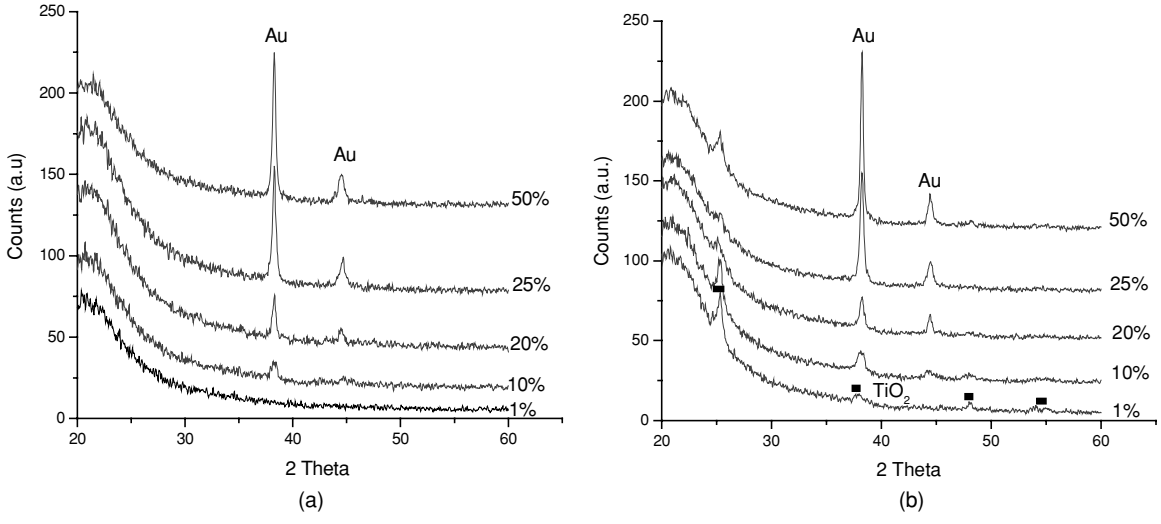


**Fig. 1** XRD spectra of Au/$TiO_2$ composite films before (a) and after (b) sintering

3.2 UV-vis optical absorption

All the $Au/TiO_2$ composite films, except the 1 at% $Au/TiO_2$, showed an obvious SPR peak in the visible region (Fig. 4) that was red-shifted with increasing Au concentrations. This red-shift was consistent with Mie's theory in which SPR performance is controlled by Au particle size [7]. It is also worth noting that the SPR peak was sharpest at low Au

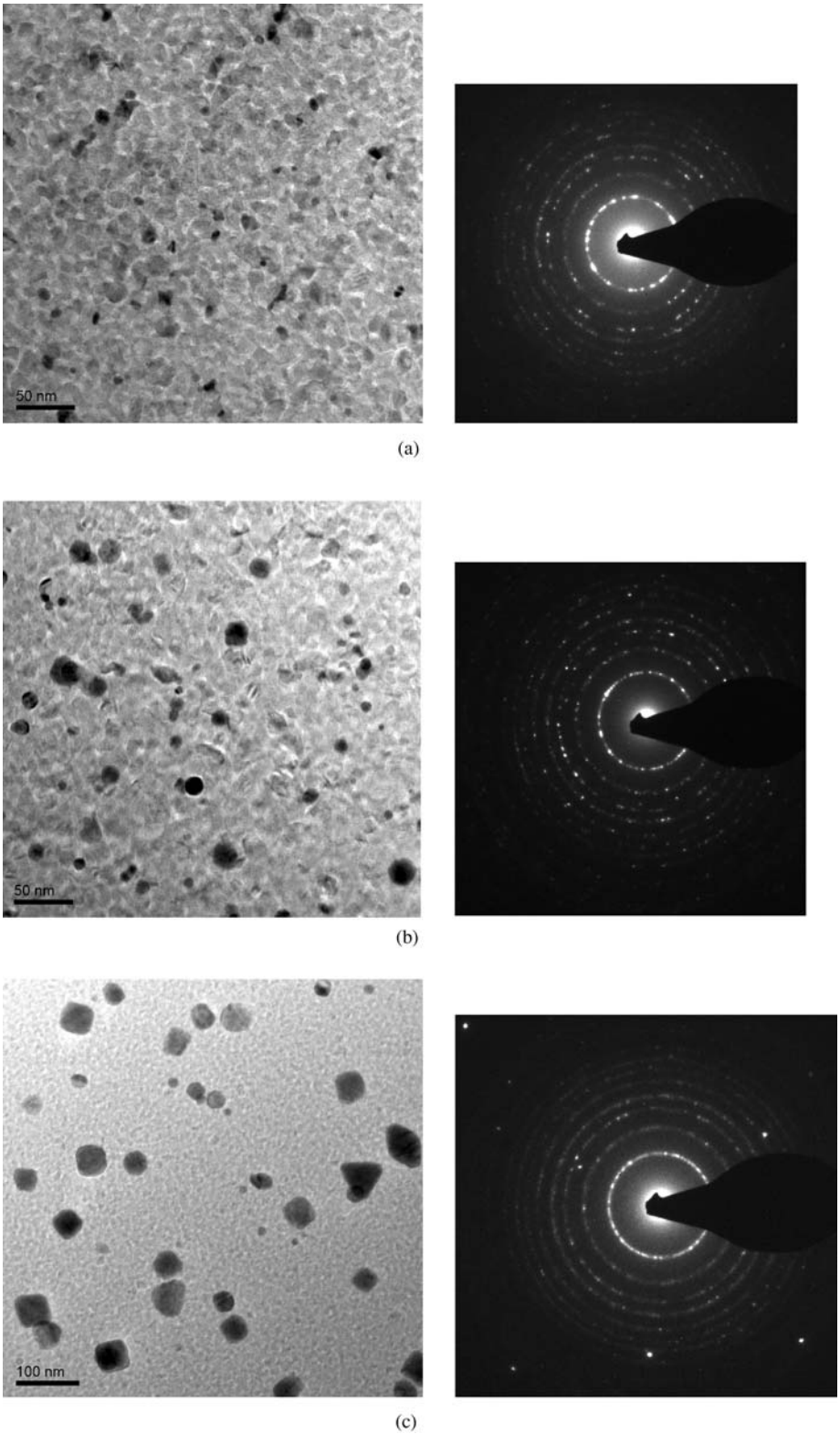


**Fig. 2** TEM images and diffraction patterns of $Au/TiO_2$ composite films with different Au concentrations. (a) 1% (b) 10% (c) 20% (d) 25% (e) 50%
*(Continued on next page.)*

**Fig. 2** *(Continued)*

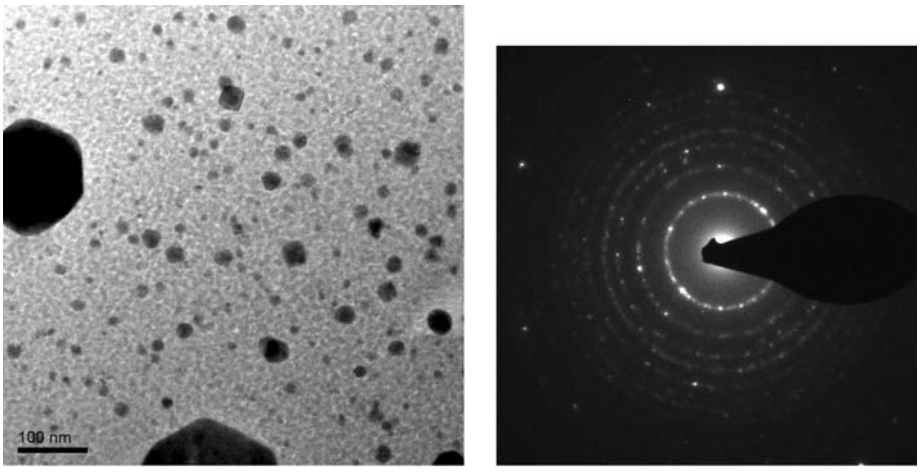


(d)

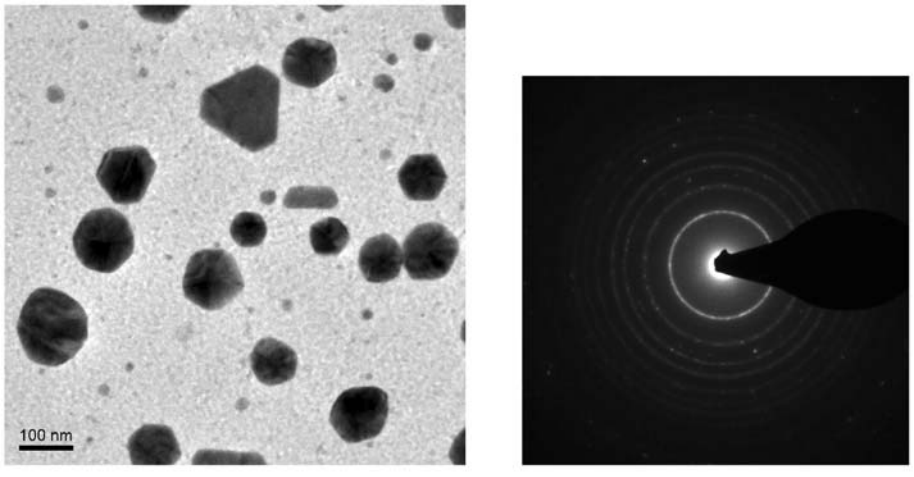


(e)

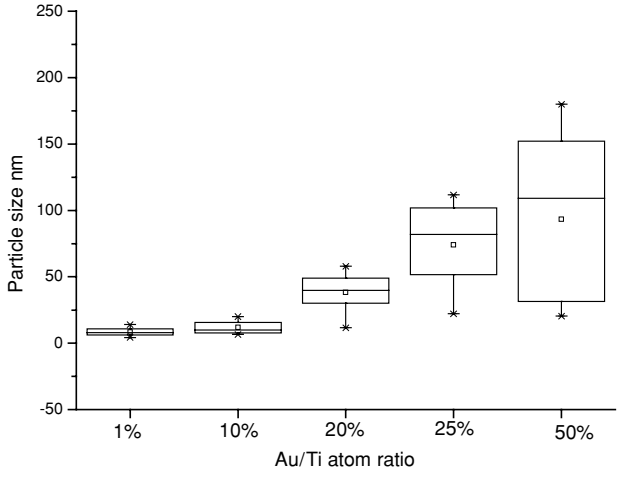


**Fig. 3** Statistical particle size distribution of $Au/TiO_2$ composite film with different Au concentrations

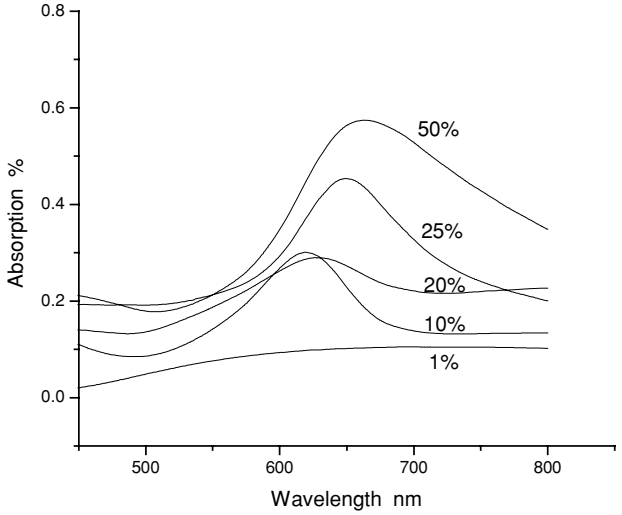


**Fig. 4** UV-vis spectra of $Au/TiO_2$ composite films with different Au/Ti atomic ratios after 500°C sintering

concentrations but its intensity was strongest at high Au concentrations. Since SPR is a collective property of the Au nanoparticles this behavior can be explained by a broad dispersion of particle size, which was indeed observed under the TEM (Fig. 2). In composite films with high Au concentrations the particle size varied from 20 to 200 nm, causing the observed broad SPR peak. The TEM also revealed that with high Au concentrations the distance between Au particles was less than that in dilute composite films, thus the interface effects between Au particles cannot be ignored. Furthermore, XRD showed that the extent of $TiO_2$ crystallization decreased at higher Au levels (Fig. 1). These results indicate that the SPR performance of the Au/$TiO_2$ composites does not only depend on the Au particle sizes, as described in Mie's theory, but also related to the interface effects between both Au-Au particles and Au-$TiO_2$ particles. This is consistent with Ung et al.'s effective medium theory, which is an extension of Mie's theory [8].

### 3.3 Photon-electron conversion

The photon-electron conversion was evaluated from photocurrents generated at composite films synthesized on ITO glasses. It was found that the photocurrent in UV region, which is mainly generated by the wide bandgap $TiO_2$, decreased with increasing Au concentrations (Fig. 5(a)). This could simply be due to Au particles blocking part of the UV light from reaching the $TiO_2$ film. However, even only a 1 at% addition of Au particles resulted in 50% reduction in the magnitude of the photocurrent peak, which suggests that additional processes besides simple light blocking contributed to the loss. It was also found that the photocurrent edge in the visible region was blue-shifted with increasing Au concentration (Fig. 5(b)). A similar blue-shift with increasing Au concentration was also found in the optical absorption edge in the region below 400 nm. These blue-shifts may be due to the weaker crystallization of the $TiO_2$ at high Au concentrations, which was observed by XRD. Bulk recombination effects are known to reduce the effective photocurrents observed from amorphous materials [9, 10], so this may explain why even 1 at% Au caused a significant drop in the photocurrent collected under UV illumination.

No obvious contribution from the SPR of the Au nanoparticles could be found in the photocurrent in the visible region, even at high Au concentrations when the SPR observed in the absorption spectra was strong. However, SPR only involves incoming photon promoting electron-hole separation, which is only the first step in photocurrent production at the Au/$TiO_2$ composite film. To produce a photocurrent the excited electrons and holes need to be transferred across the whole film. However, because of the difference in the Fermi levels between the $TiO_2$ and Au particles, a barrier exists at their interface, which the excited electrons must overcome before they can contribute to the photocurrent. Since very few of the SPR generated electrons have sufficient energy to overcome this Schottky barrier, the photocurrent is quite low in the visible region [11].

## 4 Conclusion

Au/$TiO_2$ composite films synthesized by sol-gel method were employed in an attempt to improve the photon-electron conversion efficiency of $TiO_2$ film in the visible region, using the surface plasma resonance (SPR) of Au nanoparticles.

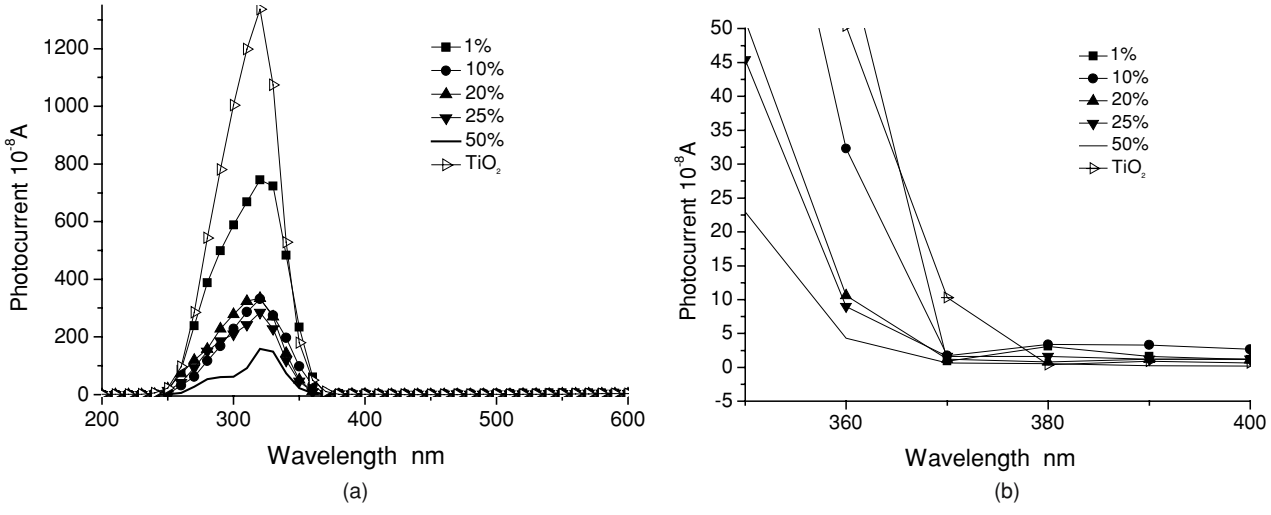


**Fig. 5** Photocurrent of Au/$TiO_2$ composite films with different Au concentrations, photocurrent edge in the visible region was illustrated in the inset graph

It was found that increasing Au concentration reduced the extent of the crystallization of the $TiO_2$, even after 500°C post-annealing, leaving some of $TiO_2$ in amorphous state. It was shown that SPR performance of the Au nanoparticles was not only related to their size, but also to their distribution in the $TiO_2$ matrix. Even in $TiO_2$ film with large Au particle sizes (10 nm), SPR in visible region was still observed. However, this did not contribute to the photon-electron conversion of $TiO_2$ film in the visible region, which suggests very few of the SPR generated electrons have sufficient energy to overcome the Schottky barrier at the Au-$TiO_2$ interface.

Unfortunately, the photocurrent from $TiO_2$ films in the UV region of the spectrum decreased with increasing levels of Au nanoparticles. The reason for this decrease is thought to be due to a combination of the aggregated Au particles physically blocking the illumination and increased bulk recombination rates, caused by the more amorphous nature of the films formed at high Au levels. In addition, this depressed crystallization was also found to blue-shift the photocurrent absorption edge in the UV region of the spectrum.

**Acknowledgment** Xiaoping Hu was supported by the NUS postgraduate research scholarship.

## References

1. J. Grunwaldt and A. Baiker, *J. Phys. Chem. B*, **103**, 1002 (1999).
2. M. Harada, F. Matsumoto, K. Nishio, and H. Masuda, *Electr. Solid State Lett.*, **8**, E27 (2005).
3. Y. Iizuka, T. Tode, and T. Takao, *J. Catal.*, **187**, 50 (1999).
4. V. Subramanian, E.E. Wolf, and P.V. Kamat, *J. Amer. Chem. Soc.*, **126**, 4943 (2004).
5. M. Takahashi, K. Tsukigi, T. Uchino, and T. Yoko, *Thin Solid Films*, **388**, 231 (2001).
6. H. Christopher, *The Basics of Crystall. Diffr.* (Oxford University Press, New York, 1997), p. 145.
7. U. Kreibig and M. Vollmer, *Optical Properties of Metal Clusters* (Springer, Berlin, 1995), p. 25.
8. T. Ung, L.M. Liz-marzan, and P. Mulvaney, *J. Phys. Chem. B*, **105**, 3441 (2001).
9. J. Bisquert, A. Zaban, and P. Salvador, *J. Phys. Chem. B*, **106**, 8774 (2002).
10. D.J. Blackwood and L.M. Peter, *Electrochimica Acta.*, **34**, 1505 (1989).
11. G. Zhao, H. Kozuka, and T. Yoko, *Thin Solid Films*, **277**, 147 (1996).